Li-Supplemental Fig. 1

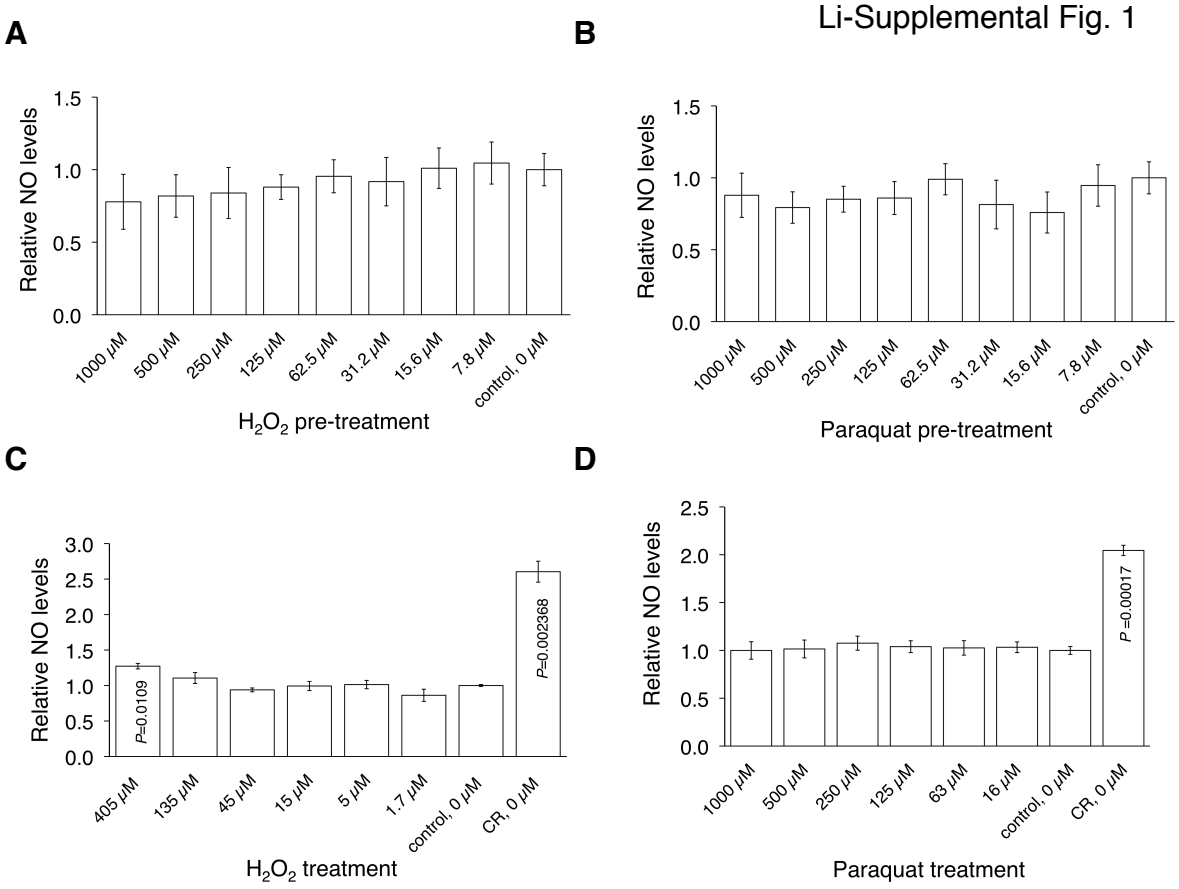

## SUPPLEMENTARY FIGURE LEGENDS

**Supplemental Fig. 1** Specificity analysis of the DAF-FM DA dye *in vivo*. Cells pre-treated with (A) hydrogen peroxide or (B) paraquat (superoxide anions) do not show increased NO-related signals. (C) and (D) Continued treatment of hydrogen peroxide and paraquat also do not increase NO-related signals. Conversely, cells grown under CR show significant increase in NO-related signals. Together these data suggest DAF-FM DA is unlikely to cross-react with hydrogen peroxide or superoxide anions or their oxidation products *in vivo* at the concentrations we tested. Activation of DAF-FA DA *in vivo* normally requires non-specific intracellular esterases. Pre-activated DAF-FA DA is therefore used in these experiments (C and D) to measure the background signals resulting from *in vitro* ROS and DAF-FA interactions. Results show NO signals in cells treated with indicated conditions with the background signals subtracted. It is noteworthy that CR still shows increased NO signals using pre-activated dye (C and D) indicating CR does not increase false-positive NO signals through activating intracellular esterases. DAF-FM (the active form of DAF-FM DA) is obtained by alkali hydrolysis of DAF-FM-DA. In brief, 5 $\mu$L of 5 mM DAF-FM DA solution in DMSO was added with 5 $\mu$L of methanol and 10 $\mu$L of 2 M NaOH and incubated at room temperature for 1 h. To the mixture, 20 $\mu$L of 2 M sodium phosphate buffer, pH 7, and 10 $\mu$L of 2 M HCL were added to obtain DAF-FM. DAF-FM was kept on ice and used on the day of preparation. *P* values were calculated using the Student's *t* test. One representative set of three independent experiments, each conducted in quadruplicate, is shown. Error bars denote standard deviations.

**Supplementary Table 1** List of mutants with increased NO levels

| Deletions | NO[a] Ave | NO[a] Std | Growth[b] (%) | Resistance[c] to GSNO (%) | CLS[d] | RLS[e] | Biological function of the gene product |
|---|---|---|---|---|---|---|---|
| *tor1Δ* | 1.60 | 0.08 | 93 | 207 | $E^{R}$ | $E^{R}$ | PIK-related protein kinase and rapamycin target |
| *fmp37*Δ | 1.48 | 0.17 | 85 | 175 | | | Biological_process unknown |
| *sto1*Δ | 1.47 | 0.18 | 77 | 175 | | | Nuclear mRNA splicing, via spliceosome |
| *smi1*Δ | 1.47 | 0.28 | 83 | 168 | | | Cell wall organization and biogenesis |
| *rgt2*Δ | 1.47 | 0.27 | 103 | 155 | | | Plasma membrane glucose receptor |
| *ctf8*Δ | 1.46 | 0.24 | 76 | 155 | | | Sister chromatid cohesion |
| *rpl13a*Δ | 1.46 | 0.12 | 79 | 173 | | $E^{R}$ | Protein component of the large (60S) ribosomal subunit |
| *cch1*Δ | 1.46 | 0.22 | 78 | 161 | | | Calcium ion transport |
| *fks1*Δ | 1.42 | 0.06 | 82 | 169 | | | Cell wall organization and biogenesis |
| *yml007c-a*Δ | 1.38 | 0.08 | 100 | 154 | | | Biological_process unknown |
| *ylr235c*Δ | 1.38 | 0.18 | 77 | 152 | | | Partially overlaps the verified gene TOP3 |
| *vps5*Δ | 1.35 | 0.14 | 82 | 154 | | | Protein-Golgi retention |
| *wsc3*Δ | 1.33 | 0.20 | 96 | 152 | | | Cell wall organization and biogenesis |
| *lst4*Δ | 1.33 | 0.17 | 100 | 155 | | | Vesicle-mediated transport |
| *cpr7*Δ | 1.30 | 0.10 | 80 | 209 | | | Peptidyl-prolyl cis-trans isomerase |
| *rps19b*Δ | 4.60 | 2.60 | 53 | 177 | | | Protein component of the small (40S) ribosomal subunit. |
| *gas1*Δ | 3.90 | 1.30 | 55 | 195 | | | Beta-1,3-glucanosyltransferase, required for cell wall assembly |
| *ykl118w*Δ | 3.70 | 0.60 | 54 | 168 | | | Overlaps the verified ORF PGD1 |
| *arv1*Δ | 3.30 | 0.80 | 41 | 176 | | | Intracellular sterol distribution |
| *tpd3*Δ | 2.90 | 0.50 | 28 | 158 | | | Regulatory subunit A of the heterotrimeric protein phosphatase 2A |
| *spt21*Δ | 2.80 | 0.50 | 62 | 168 | | | Regulation of transcription from Pol II promoter |
| *nup84*Δ | 2.70 | 0.30 | 56 | 154 | | | mRNA-nucleus export |
| *nsr1*Δ | 2.60 | 1.00 | 45 | 177 | | | Pre-rRNA processing and ribosome biogenesis |
| *rpl13b*Δ | 2.60 | 0.30 | 58 | 141 | | | Protein component of the large (60S) ribosomal subunit |
| *ykl118w*Δ | 2.60 | 0.60 | 48 | 155 | | | Overlaps the verified gene VPH2 |
| *hhf2*Δ | 2.60 | 0.60 | 64 | 155 | E(0.02) | | One of two identical histone H4 proteins; involved in chromatin assembly |
| *erg6*Δ | 2.50 | 0.40 | 61 | 178 | | | Ergosterol biosynthesis |
| *vph2*Δ | 2.40 | 0.70 | 48 | 146 | | | Assembly of the V-ATPase; |

| | | | | | | |
|---|---|---|---|---|---|---|
| *tom5*Δ | 2.40 | 0.40 | 62 | 135 | | Import of proteins into mitochondria |
| *lsm6*Δ | 2.30 | 0.30 | 63 | 165 | | Nuclear mRNA splicing, via spliceosome |
| *pgd1*Δ | 2.30 | 0.50 | 56 | 163 | | Subunit of the RNA polymerase II mediator complex |
| *htl1*Δ | 2.20 | 0.80 | 69 | 162 | | Regulation of cell cycle |
| *shp1*Δ | 2.20 | 0.90 | 38 | 165 | | Interacts with ubiquitylated proteins and is required for degradation of a ubiquitylated model substrate. |
| *yel059w*Δ | 2.20 | 0.30 | 66 | 190 | | Biological_process unknown |
| *ssn2*Δ | 2.20 | 0.60 | 57 | 163 | $E^R$ | Negative regulation of transcription from Pol II promoter |
| *bud22*Δ | 2.20 | 0.50 | 43 | 187 | | Bud site selection |
| *vma6*Δ | 2.10 | 0.40 | 58 | 133 | | Subunit d of the five-subunit V0 integral membrane domain of vacuolar H+-ATPase. Vacuolar acidification |
| *sec22*Δ | 2.10 | 0.10 | 48 | 159 | | ER to Golgi transport |
| *tsr2*Δ | 2.10 | 0.70 | 41 | 169 | | Processing of pre-rRNA |
| *ngl1*Δ | 2.10 | 0.50 | 108 | 141 | | Biological_process unknown |
| *mms22*Δ | 2.00 | 0.70 | 55 | 154 | | Double-strand break repair |
| *sec28*Δ | 2.00 | 0.50 | 59 | 166 | | ER to Golgi transport |
| *qcr7*Δ | 2.00 | 0.50 | 73 | 129 | | Aerobic respiration |
| *ccr4*Δ | 2.00 | 0.30 | 46 | 146 | | Regulation of transcription from Pol II promoter |
| *adh3*Δ | 2.00 | 0.30 | 84 | 148 | | Mitochondrial alcohol dehydrogenase isozyme III. |
| *thp1*Δ | 2.00 | 0.20 | 57 | 151 | | Involved in transcription and in mRNA export from the nucleus |
| *msn5*Δ | 1.90 | 0.70 | 98 | 138 | | Protein-nucleus export |
| *cup5*Δ | 1.90 | 0.20 | 36 | 149 | | Proteolipid subunit of the vacuolar H(+)-ATPase V0 sector |
| *vps64*Δ | 1.90 | 0.40 | 59 | 123 | | Cytoplasmic protein required for cytoplasm to vacuole targeting of proteins. |
| *ctk3*Δ | 1.90 | 0.50 | 17 | 161 | | Gamma subunit of C-terminal domain kinase I. Affect both transcription and pre-mRNA 3' end processing. |
| *mct1*Δ | 1.90 | 0.40 | 78 | 127 | | Predicted malonyl-CoA:ACP transferase, putative component of a type-II mitochondrial fatty acid synthase that produces intermediates for phospholipid remodeling. |
| *rpl36b*Δ | 1.90 | 0.30 | 45 | 193 | | Protein component of the large (60S) ribosomal subunit |
| *ynr068c*Δ | 1.80 | 0.20 | 71 | 147 | | Biological_process unknown |
| *ygr160w*Δ | 1.80 | 0.10 | 47 | 194 | | Biological_process unknown |
| *yjl046w*Δ | 1.80 | 0.60 | 128 | 106 | | Biological_process unknown |
| *def1*Δ | 1.81 | 0.50 | 46 | 176 | | Ubiquitin-dependent protein catabolism |

| | | | | | |
|---|---|---|---|---|---|
| *sum1*Δ | 1.80 | 0.47 | 101 | 144 | Chromatin silencing at telomere |
| *rps16b*Δ | 1.79 | 0.02 | 64 | 164 | Protein component of the small (40S) ribosomal subunit |
| *efg1*Δ | 1.77 | 0.35 | 59 | 181 | Essential protein required for maturation of 18S rRNA |
| *lea1*Δ | 1.76 | 0.69 | 38 | 159 | Nuclear mRNA splicing, via spliceosome |
| *idh1*Δ | 1.73 | 0.20 | 51 | 203 | Subunit of mitochondrial NAD(+)-dependent isocitrate dehydrogenase, which catalyzes the oxidation of isocitrate to alpha-ketoglutarate in the TCA cycle |
| *hfa1*Δ | 1.72 | 0.66 | 135 | 99 | Mitochondrial acetyl-coenzyme A carboxylas |
| *gcn20*Δ | 1.72 | 0.35 | 45 | 157 | Proposed to stimulate Gcn2p activation by an uncharged tRNA |
| *erg3*Δ | 1.71 | 0.36 | 58 | 166 | Ergosterol biosynthesis |
| *hmg1*Δ | 1.70 | 0.2 | 84 | 175 | HMG-CoA reductase, catalyzes the rate-limiting step in sterol biosynthesis |
| *gcv3*Δ | 1.70 | 0.39 | 83 | 130 | One-carbon compound metabolism |
| *ydj1*Δ | 1.70 | 0.30 | 72 | 153 | Protein chaperone involved in regulation of the HSP90 and HSP70 functions |
| *rps28b*Δ | 1.68 | 0.65 | 73 | 157 | Protein component of the small (40S) ribosomal subunit |
| *ald4*Δ | 1.68 | 0.06 | 129 | 120 | Mitochondrial aldehyde dehydrogenase, required for growth on ethanol and conversion of acetaldehyde to acetate. |
| *rps10a*Δ | 1.67 | 0.31 | 63 | 141 | Protein component of the small (40S) ribosomal subunit |
| *med2*Δ | 1.67 | 0.34 | 53 | 164 | Subunit of the RNA polymerase II mediator complex |
| *rad50*Δ | 1.64 | 0.31 | 69 | 145 | Double-strand break repair via nonhomologous end-joining |
| *num1*Δ | 1.62 | 0.23 | 45 | 168 | Nuclear migration |
| *sgf73*Δ | 1.62 | 0.34 | 71 | 124 | Histone acetylation |
| *swd1*Δ | 1.61 | 0.41 | 105 | 134 | Chromatin silencing at telomere |
| *sac1*Δ | 1.61 | 0.30 | 66 | 176 | Involved in protein trafficking and processing, secretion, and cell wall maintenance |
| *ldb18*Δ | 1.57 | 0.33 | 37 | 159 | biological_process unknown |
| *arp1*Δ | 1.57 | 0.12 | 34 | 149 | Actin-related protein of the dynactin complex |
| *rps16a*Δ | 1.56 | 0.27 | 53 | 181 | Protein component of the small (40S) ribosomal subunit |
| *sli15*Δ | 1.56 | 0.07 | 82 | 146 | Subunit of the Ipl1p-Sli15p-Bir1p complex that regulates kinetochore-microtubule attachments |

| | | | | | | |
|---|---|---|---|---|---|---|
| *ypl205c*Δ | 1.55 | 0.10 | 64 | 177 | | Deletion of locus affects telomere length |
| *snf6*Δ | 1.55 | 0.23 | 70 | 140 | | Subunit of the SWI/SNF chromatin remodeling complex |
| *est3*Δ | 1.53 | 0.13 | 62 | 165 | | Telomerase-dependent telomere maintenance |
| *rps1b*Δ | 1.52 | 0.03 | 58 | 191 | | Protein component of the small (40S) ribosomal subunit |
| *rps27b*Δ | 1.52 | 0.08 | 67 | 131 | | Protein component of the small (40S) ribosomal subunit |
| *rpl37a*Δ | 1.52 | 0.12 | 70 | 151 | | Protein component of the large (60S) ribosomal subunit |
| *arc18*Δ | 1.51 | 0.34 | 91 | 140 | | Actin filament organization |
| *scs7*Δ | 1.51 | 0.13 | 85 | 131 | | Sphingolipid alpha-hydroxylase, functions in the alpha-hydroxylation of sphingolipid-associated very long chain fatty acids |
| *ydr149c*Δ | 1.51 | 0.00 | 43 | 175 | | Overlap with NUM1 |
| *erg24*Δ | 1.50 | 0.08 | 65 | 169 | | Ergosterol biosynthesis |
| *asc1*Δ | 1.49 | 0.32 | 57 | 169 | | Core component of the small (40S) ribosomal subunit |
| *rmr1*Δ | 1.49 | 0.22 | 50 | 173 | | Protein required for meiotic recombination and gene conversion |
| *she3*Δ | 1.48 | 0.21 | 82 | 113 | | mRNA localization, intracellular |
| *ynl311c*Δ | 1.48 | 0.11 | 56 | 195 | | Ubiquitin-dependent protein catabolism |
| *gcn3*Δ | 1.45 | 0.07 | 72 | 113 | | Translational initiation |
| *bem2*Δ | 1.43 | 0.23 | 72 | 156 | | Control of cytoskeleton organization and cellular morphogenesis |
| *vma9*Δ | 1.43 | 0.31 | 38 | 142 | | Vacuolar H+ ATPase subunit e of the V-ATPase V0 subcomplex |
| *vam10*Δ | 1.42 | 0.12 | 77 | 146 | | Vacuole fusion (non-autophagic) |
| *pkh2*Δ | 1.41 | 0.20 | 125 | 121 | E(0.0035) | Serine/threonine protein kinase |
| *sac6*Δ | 1.41 | 0.15 | 57 | 154 | | Organization and maintenance of the actin cytoskeleton |
| *rlf2*Δ | 1.41 | 0.22 | 100 | 142 | | Nucleosome assembly |
| *vam7*Δ | 1.40 | 0.26 | 43 | 179 | | Component of the vacuole SNARE complex involved in vacuolar morphogenesis |
| *bub3*Δ | 1.40 | 0.22 | 54 | 141 | | Kinetochore checkpoint WD40 repeat protein |
| *cdh1*Δ | 1.39 | 0.16 | 65 | 150 | | Cell-cycle regulated activator of the anaphase-promoting complex/cyclosome |
| *ydr199w*Δ | 1.39 | 0.10 | 91 | 143 | | Overlap with VPS64 |
| *lst7*Δ | 1.39 | 0.06 | 91 | 130 | $E^R$ | Vesicle-mediated transport |
| *dbf2*Δ | 1.37 | 0.27 | 83 | 133 | | Ser/Thr kinase involved in transcription and stress response |
| *bst1*Δ | 1.36 | 0.09 | 72 | 159 | $E^R$ | ER-associated protein catabolism |

| | | | | | | | |
|---|---|---|---|---|---|---|---|
| *rfm1*Δ | 1.34 | 0.10 | 91 | 147 | | | DNA-binding protein required for vegetative repression of middle sporulation genes |
| *top3*Δ | 1.34 | 0.15 | 72 | 146 | | | DNA Topoisomerase III, involved in telomere stability and regulation of mitotic recombination. |
| *yhi9*Δ | 1.34 | 0.29 | 70 | 170 | | | Biological_process unknown |
| *ybr196c-a*Δ | 1.34 | 0.15 | 62 | 161 | | | Biological_process unknown |
| *vps8*Δ | 1.34 | 0.15 | 69 | 154 | | | Membrane-associated protein that interacts with Vps21p to facilitate soluble vacuolar protein localization |
| *isc1*Δ | 1.33 | 0.13 | 34 | 166 | | | Salinity response |
| *plc1*Δ | 1.33 | 0.16 | 38 | 164 | | | Phospholipase C, hydrolyzes phosphatidylinositol 4,5-biphosphate (PIP2) to generate the signaling molecules inositol 1,4,5-triphosphate (IP3) |
| *vid21*Δ | 1.32 | 0.11 | 59 | 137 | | | Component of the NuA4 histone acetyltransferase complex |
| *ymr052c-a*Δ | 1.31 | 0.07 | 56 | 163 | | | Biological_process unknown |
| *rrp8*Δ | 1.31 | 0.10 | 66 | 165 | | $E^R$ | Nucleolar protein involved in rRNA processing |
| *ssd1*Δ | 1.30 | 0.01 | 99 | 142 | | | Protein with a role in maintenance of cellular integrity, interacts with components of the TOR pathway |
| *rps24a*Δ | 1.30 | 0.19 | 64 | 184 | | | Protein component of the small (40S) ribosomal subunit |
| *yml013c-a*Δ | 1.29 | 0.12 | 82 | 139 | | | Biological_process unknown |
| *she4*Δ | 1.29 | 0.05 | 74 | 126 | | | Protein containing a UCS (UNC-45/CRO1/SHE4) domain, binds to myosin motor domains to regulate myosin function |
| *ybr174c*Δ | 1.28 | 0.09 | 84 | 143 | | | Biological_process unknown |
| *vps9*Δ | 1.27 | 0.07 | 124 | 113 | | | A guanine nucleotide exchange factor involved in vesicle-mediated vacuolar protein transport |
| *tma23*Δ | 1.26 | 0.12 | 67 | 191 | | | Nucleolar protein of unknown function implicated in ribosome biogenesis |
| *hxt17*Δ | 1.26 | 0.10 | 125 | 120 | E(0.0004) | | Hexose transporter |
| *vps51*Δ | 1.26 | 0.12 | 63 | 167 | | | Required for the recycling of proteins from endosomes to the late Golgi |
| *rps18b*Δ | 1.26 | 0.03 | 54 | 169 | | | Protein component of the small (40S) ribosomal subunit |
| *pkr1*Δ | 1.25 | 0.15 | 90 | 116 | | | V-ATPase assembly factor |
| *ygl088w*Δ | 1.24 | 0.18 | 62 | 167 | | | Biological_process unknown |
| *rpl14a*Δ | 1.24 | 0.15 | 74 | 140 | | | Protein component of the large |

| | | | | | | |
|---|---|---|---|---|---|---|
| | | | | | | (60S) ribosomal subunit |
| *ydl063c*Δ | 1.24 | 0.08 | 79 | 169 | | Biological_process unknown |
| *fyv12*Δ | 1.24 | 0.13 | 34 | 172 | | Biological_process unknown |
| *rps19a*Δ | 1.23 | 0.02 | 57 | 175 | | Protein component of the small (40S) ribosomal subunit |
| *tna1*Δ | 1.23 | 0.14 | 56 | 159 | | Nicotinic acid transport |
| *glg2*Δ | 1.23 | 0.11 | 92 | 122 | | Glycogen biosynthesis |
| *ckb1*Δ | 1.21 | 0.07 | 70 | 161 | | Ser/Thr protein kinase with roles in cell growth and proliferation |
| *srb5*Δ | 1.21 | 0.13 | 63 | 150 | | Transcription from Pol II promoter |
| *seh1*Δ | 1.21 | 0.09 | 73 | 163 | | Nuclear pore protein that is part of the evolutionarily conserved Nup84p complex |
| *rpl20b*Δ | 1.21 | 0.14 | 72 | 138 | $E^R$ | Protein component of the large (60S) ribosomal subunit |
| *rpl31a*Δ | 1.20 | 0.06 | 79 | 172 | | Protein component of the large (60S) ribosomal subunit |

This table lists top 16 to 157 hits from our screen (Top 1-15 hits are shown in **Table 1**). Among mutants listed here, the first 16 (top 16-31 hits) were first selected by their "Growth[b]" (at least 75% of WT; no severe growth defects) and by "Resistance[c] to GSNO" (at least 150% of WT), then were ranked by NO levels. The remaining mutants (31-157) were ranked by NO levels only.

[a] Numbers show relative average NO levels (Ave) and standard deviations (Std) from three sets of experiments. Average NO levels are normalized to that of wild type cells, which are set to 1. Mutants with NO levels ≥1.2 are shown.

[b] Numbers show the percentage of cell growth normalized to that of wild type cells which is set to 100%. Cell growth is monitored for 8 hours at staring $OD_{600}$ of 0.1.

[c] Numbers show the percentage of cell growth normalized to that of wild type cells which is set to 100% in growth media containing 200 $\mu$M GSNO. Cell growth is monitored for 8 hours at staring $OD_{600}$ of 0.1. Mutant with growth rate ≥100% are shown.

[d] CLS, chronological life span. E: extended; (*P*-values) are calculated using the AUC (area under curve) method; $E^R$: reported to extend life span (Powers R. W. et al, 2006, *Genes Dev* **20**:174-184; Bonawitz N. D. et al, 2007, *Cell Metab* **5**:265-277; Wang C., et al, 2009, *Genetics* **183**:1373-1384).

[e] RLS, replicative life span. $E^R$: reported to extend life span (Kaeberlein M. et al, 2005, *Science* **310**:1193-1196; Steffen K. K. et al, 2008, *Cell* **133**:292-302).

**Supplemental Table 2** Pair-wise statistical analysis of chronological life span (CLS)

| Figures | Strains | P value |
|---|---|---|
| Fig. 2A | WT[a] vs CR[b] | P=0.0004 |
| | WT vs *hxt17*Δ | P=0.0004 |
| | *hxt17*Δ vs *hxt17*Δ, CR | P=0.1496 (NS[c]) |
| | CR vs *hxt17*Δ, CR | P=0.1377 (NS) |
| | WT vs *pkh2*Δ | P=0.0035 |
| | *pkh2*Δ vs *pkh2*Δ, CR | P=0.1599 (NS[c]) |
| | CR vs *pkh2*Δ, CR | P=0.145 (NS) |
| Fig. 2B | WT vs CR | P=0.0048 |
| | WT vs *soy1*Δ | P=0.0024 |
| | *soy1*Δ vs *soy1*Δ, CR | P=0.173 (NS) |
| | CR vs *soy1*Δ, CR | P=0.098 (NS) |
| Fig. 2C | WT vs CR | P=0.0205 |
| | WT vs *gup1*Δ | P=0.0261 |
| | *gup1*Δ vs *gup1*Δ, CR | P=0.0352 |
| | CR vs *gup1*Δ, CR | P=0.0725 (NS) |
| Fig. 2D | WT vs CR | P=0.0021 |
| | WT vs *hhf1*Δ | P=0.00534 |
| | *hhf1*Δ vs *hhf1*Δ, CR | P=0.0203 |
| | CR vs *hhf1*Δ, CR | P=0.28 (NS) |
| Fig. 4B | WT vs CR | P=0.0005 |
| | WT vs *cyt1*Δ | P<0.0001 |
| | *cyt1*Δ vs *cyt1*Δ, CR | P=0.241 (NS) |
| | CR vs *cyt1*Δ, CR | P=0.00012 |
| Fig. 5D | WT vs CR | P=0.0145 |
| | WT vs *sfa1*Δ*yhb1*Δ | P=0.4273 (NS) |
| | *sfa1*Δ*yhb1*Δ vs *sfa1*Δ*yhb1*Δ, CR | P=0.0085 |
| | CR vs *sfa1*Δ*yhb1*Δ, CR | P=0.5372 (NS) |
| Fig. 6A | no treatment vs buffer only | P=0.09586 (NS) |
| | no treatment vs inactivated GSNO | P=0.5507 (NS) |
| | buffer only vs GSNO (25 μM) | P=0.0016 |
| | buffer only vs CR +buffer | P=0.0027 |
| | GSNO vs CR+GSNO | P=0.6366 (NS) |
| | CR vs CR+GSNO | P=0.6111 (NS) |
| | CR vs CR+inactivated GSNO | P=0.9557 (NS) |
| Fig. 6B | no treatment vs buffer only | P=0.45 (NS) |
| | no treatment vs inactivated GSNO | P=0.14 (NS) |
| | buffer only vs GSNO (5 μM, 6x) | P<0.0001 |
| | buffer only vs CR +buffer | P<0.0001 |
| | GSNO vs CR+GSNO | P=0.01 |
| | CR vs CR+GSNO | P=0.5 (NS) |
| | CR vs CR+inactivated GSNO | P=0.64 (NS) |
| Fig. 6C | WT vs GSNO | P=0.0069 |
| | WT vs *pkh2*Δ | P=0.0057 |
| | WT vs *hxt17*Δ | P=0.013 |
| | WT vs *hhf1*Δ | P=0.0085 |
| | *pkh2*Δ vs *pkh2*Δ+GSNO | P=0.4383 (NS) |

| Figures | Strains | P value |
|---|---|---|
| Fig. 6C | *hxt17*Δ vs *hxt17*Δ+GSNO | P=0.3922 (NS) |
| | *hhf1*Δ vs *hhf1*Δ+GSNO | P=0.5405 (NS) |

Statistical analyses are carried out using the AUC method (area under the curve) (Pruessner J. C. et al, 2003, Psychoneuroendocrinology 28:916-931; Fekedulegn D. B. et al, 2007, Psychosom Med 69:651-659). *P*-values were calculated for each pair of lifespan. 3-4 independent colonies derived from each strain were analyzed in each experiment. About $2x10^8$ cells were analyzed for each sample in each experiment. WT[a]: BY4742; CR[b]: calorie restriction; NS[c]: not significant.

**Supplemental Table 3** Pair-wise statistical analysis of replicative life span (RLS)

| Figures | Strains | P value |
|---|---|---|
| Fig. 3A | WT[a] vs CR[b] | P=0.0017 |
| | WT vs *hxt17*Δ | P<0.0014 |
| | *hxt17*Δ vs *hxt17*Δ, CR | P=0.3962 (NS[c]) |
| | CR vs *hxt17*Δ, CR | P=0.2536 (NS) |
| | WT vs *pkh2*Δ | P=0.0001 |
| | *pkh2*Δ vs *pkh2*Δ, CR | P=0.8740 (NS) |
| | CR vs *pkh2*Δ, CR | P=0.3376 (NS) |
| Fig. 3B | WT vs CR | P=0.003 |
| | WT vs *soy1*Δ | P<0.0001 |
| | *soy1*Δ vs *soy1*Δ, CR | P=0.0083 |
| | CR vs *soy1*Δ, CR | P=0.4947 (NS) |
| Fig. 3C | WT vs CR | P=0.0004 |
| | WT vs *gup1*Δ | P=0.0001 |
| | *gup1*Δ vs *gup1*Δ, CR | P=0.0381 |
| | CR vs *gup1*Δ, CR | P=0.0038 |
| | WT vs *ipk1*Δ | P=0.0065 |
| | *ipk1*Δ vs *ipk1*Δ, CR | P=0.3205 (NS) |
| | CR vs *ipk1*Δ, CR | P=0.7509 (NS) |
| Fig. 3D | WT vs CR | P=0.003 |
| | WT vs *hhf1*Δ | P<0.0001 |
| | *hhf1*Δ vs *hhf1*Δ, CR | P=0.1865 (NS) |
| | CR vs *hhf1*Δ, CR | P=0.0007 |
| Fig. 4C | WT vs *cyt1*Δ | P<0.0001 |
| | *cyt1*Δ vs *cyt1*Δ*hhf1*Δ | P=0.1618 (NS) |
| | *cyt1*Δ vs *cyt1*Δ*gup1*Δ | P=0.6809 (NS) |
| | *cyt1*Δ vs *cyt1*Δ*ipk1*Δ | P=0.2116 (NS) |
| | *cyt1*Δ vs *cyt1*Δ*soy1*Δ | P=0.7956 (NS) |
| Fig. 5A | WT vs CR | P<0.0001 |
| | WT vs *sfa1*Δ | P=0.5067 (NS) |
| | WT vs *yhb1*ΔΔ | P=0.3862 (NS) |
| | WT vs *sfa1*Δ*yhb1*ΔΔ | P=0.1316 (NS) |
| | *sfa1*Δ vs *sfa1*Δ, CR | P=0.0008 |
| | CR vs *sfa1*Δ, CR | P=0.1882 (NS) |
| | *yhb1*Δ vs *yhb1*Δ, CR | P=0.0504 |
| | CR vs *yhb1*Δ, CR | P=0.029 |
| | *sfa1*Δ*yhb1*Δ vs *sfa1*Δ*yhb1*Δ, CR | P=0.8528 (NS) |
| | CR vs *sfa1*Δ*yhb1*Δ, CR | P<0.0001 |
| Fig. 5B | WT vs *sfa1*Δ*yhb1*ΔΔ | P=0.6013 (NS) |
| | *sfa1*Δ*yhb1*Δ vs *hxt17*Δ*sfa1*Δ*yhb1*Δ | P=0.9436 (NS) |
| | *sfa1*Δ*yhb1*Δ vs *pkh2*Δ*sfa1*Δ*yhb1*Δ | P=0.6706 (NS) |
| | *sfa1*Δ*yhb1*Δ vs *hhf1*Δ*sfa1*Δ*yhb1*Δ | P=0.4112 (NS) |

Statistical analyses are carried out using the JMP statistics software (SAS), and Wilcoxon rank-sums tests *P*-values are calculated for each pair of lifespan. WT[a]: BY4742; CR[b]: calorie restriction; NS[c]: not significant.